In situ high-pressure X-ray diffraction experiments and *ab initio* calculations of Co_2P*

Zhang Qian(张 倩), Wu Xiang(巫 翔)†, and Qin Shan(秦 善)

Key Laboratory of Orogenic Belts and Crustal Evolution of Ministry of Education, School of Earth and Space Sciences, Peking University, Beijing 100871, *China*

(Received 2 September 2010; revised manuscript received 21 January 2011)

In situ high-pressure experiments of Co_2P are carried out by means of angle dispersive X-ray diffraction with diamond anvil cell technique. No phase transition is observed in the present pressure range up to 15 GPa at room temperature, even at high temperature and 15 GPa. Results of compression for Co_2P are well presented by the second-order Birch–Murnaghan equation of state with $V_0 = 130.99(2)$ Å^3 (1 Å=0.1 nm) and $K_0 = 160(3)$ GPa. Axial compressibilities are described by compressional modulus of the axis: $K_a = 123(2)$ GPa, $K_b = 167(8)$ GPa and $K_c = 220(7)$ GPa. Theoretical calculations further support the experimental results and indicate that C23-type Co_2P is stable at high pressure compared with the C22-type phase.

Keywords: Co_2P, *ab initio*, pressure-induced phase transition

PACS: 61.05.cp, 71.15.Nc, 91.60.Hg **DOI:** 10.1088/1674-1056/20/6/066101

1. Introduction

The 3d transition metal phosphides, M_2P (where M ranges from Mn to Ni) have been extensively investigated due to their diverse magnetic properties and typical crystal structures.[1−3] Recently, M_2P compounds have been discovered in many meteorites, such as allabogdanite.[4] Exploring the high-pressure behaviour of M_2P is therefore of significant interest in discussing phosphorus storage in planetary cores. In ambient conditions, the above compounds crystallize into two similar structures: C22-type ($P\bar{6}2m$) for Mn_2P, Fe_2P, Ni_2P; and C23-type ($Pnma$) for Co_2P. In both structures metal atoms are coordinated by phosphor atoms in two types of environments (square pyramidal CN=5 and tetrahedral CN=4). The phosphor atoms are nine-coordinate, residing in the centres of trigonal prisms formed by the metal atoms, with three additional capping metal atoms provided by neighbouring trigonal prisms.

C22-type and C23-type structures can alternate by increasing 3d electron numbers: Mn_2P (C22)–FeMnP (C23)–Fe_2P (C22)–Co_2P (C23)–Ni_2P (C22). Temperature and (or) pressure thermal parameters can also induce a phase transition between C22 and C23. For example, C22-type Fe_2P transforms into the C23-type phase at above 8 GPa and 1000 K.[5] Besides C22 and C23 polymorphs, a new high-pressure polymorph of Fe_2P was proposed with a monoclinic structure at pressure between 30 GPa and 50 GPa.[6] As an isostructural analogue of the C22-type Fe_2P, Ni_2P without heating remains stable up to at least 50 GPa.[7] Therefore, nickel was deduced to have a stabilizing effect on the C23-type phase of the $(Fe,Ni)_2P$ allabogdanite.[4] Co_2P has a C23-type structure located in the middle between Fe_2P and Ni_2P. Fifty years ago, the structure of Co_2P was refined by X-ray single crystal diffraction method,[8] showing that it represents the Co_2Si-type structure according to the crystal structure characterization.[9] A polymorphic phase transformation of Co_2P was suggested at 1193 K on the basis of thermoanalytical data.[10] The corresponding phase transformation temperature was further confirmed to be 1413 K by means of differential thermal analysis experiments.[11] The melting point of Co_2P is 1659 K.[12,13]

In contrast to Fe_2P and Ni_2P, there is no available information about the high-pressure behaviour of Co_2P. In this study, therefore, our aim is to explore the structural stability of Co_2P at high pressure by *in situ* X-ray diffraction (XRD) with diamond anvil cell (DAC). We also underpin the data by density functional theory (DFT) based on electronic structure cal-

*Project supported by the National Natural Science Foundation of China (Grant Nos. 40972029 and 41072027).

†Corresponding author. E-mail: xiang.wu@pku.edu.cn

© 2011 Chinese Physical Society and IOP Publishing Ltd

culations.

2. Experiments

The Co_2P sample used in this study was synthesized by the standard solid-state reaction. Stoichiometric amounts of Co (99.99%) and red P (99.99%) were mixed and ground in an agate mortar. The mixture was compressed into a pellet with a diameter of 3 mm, which was loaded in a sealed and evacuated quartz tube with a diameter of 4 mm. The mixture was sintered at 900 °C for 48 h. Then it was cooled down to room temperature for several hours. The product structure was characterized by conventional X-ray diffractometer with Cu target. The value of 2θ ranging from 20° to 90° was collected in steps of 0.02° in 1.5-s exposure time.

The high-pressure device in our work was a four-pin modified Merrill–Basset type DAC with 500-μm diameter culets. A 260-μm diameter hole was drilled in the pre-indented 65-μm thickness rhenium gasket. NaCl was used as a pressure-transmitting medium and an insulator. A small ruby sphere was loaded in the centre of the sample hole for pressure calibration.[14] The pressure error was estimated by comparing the value obtained from Ruby fluorescence with that from equation of state (EoS) of NaCl.[15] The high temperature was obtained by a portable laser heating for DAC, where 1064-nm laser radiation was applied.[16]

The *in situ* XRD measurements up to 15 GPa were carried out at Bayerisches Geoinstitut (Germany) using a system consisting of a high-brilliance FRD rotating anode generator and a Bruker APEX charge-coupled device area detector. An accelerating voltage of 55 kV and a beam current of 60 mA were applied. Mo Kα radiation ($\lambda = 0.7108$ Å) was focused into $\sim$ ϕ50-μm full width at half maximum (FWHM) beam in size. Collection time for each pattern was 15 min. All collected images were integrated using the Fit2D program in order to obtain conventional one-dimensional diffraction spectra. The XRD patterns were analysed by a full-profile model refinement implemented in the GSAS software.

The first-principles calculations performed in this paper are based on DFT, using the full potential linearized augmented plane wave (FPLAW) within the local spin density approximation (LSDA) plus Hubbard U, implemented in the WIEN2K code.[17,18] According to the introduction at the beginning, two candidate models were designed: C22 and C23. The muffin-tin radii of Co and P were chosen as 1.9 and 1.7 Bohr in all calculations. In the LAPW calculations, the energy threshold was set at -7.0 Ry (1 Ry=13.605 eV) between core and valence states. The muffin-tin radius multiplied by $K_{\max}$ (for the plane waves) was set to be a value of 7.0. The 500-K points were specified in the whole Brillouin zone. For each crystalline phase, we obtained the minimum total energy in a constant volume by allowing the atoms and cell geometry to relax into their lowest energy configuration, with a tolerance value taken as 1 mRy/Bohr in the self-consistency cycles. Hubbard $U = 5$ eV and $J = 0.95$ eV were used for Co atom in all LSDA+U calculations.[19]

3. Results and discussion

3.1. The X-ray powder diffraction

Figure 1 shows the X-ray diffraction pattern of Co_2P under ambient conditions, analysed by a full profile model refinement. All peaks can be indexed to the C23-type phase, indicating that the synthetic product is a single phase without any impurity. Lattice parameters ($a = 5.6510(2)$ Å, $b = 3.5090(1)$ Å, $c = 6.6054(2)$ Å, and $V = 130.983(6)$ Å^3) are well consistent with previous results ($a = 5.6479(4)$ Å, $b = 3.5129(2)$ Å, $c = 6.6078(4)$ Å, and $V = 131.10(1)$ Å^3).[20]

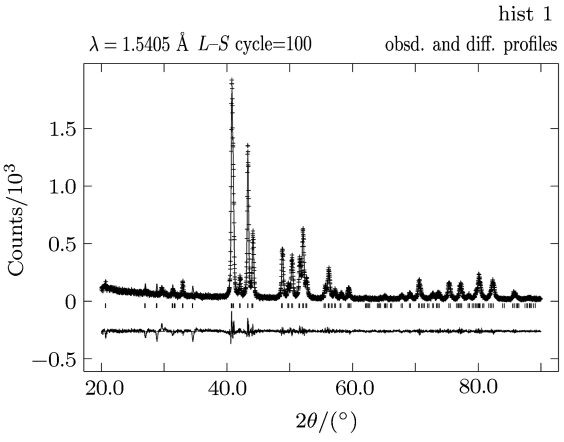


Fig. 1. Results of a full-profile model refinement under ambient conditions, where XRD pattern was recorded with Cu target. The experimental data are shown as the cross symbol, the calculated fits and difference curves as solid lines. Tick marks indicate the calculated reflection positions. Lattice parameters are $a = 5.6510(2)$ Å, $b = 3.5090(1)$ Å, $c = 6.6054(2)$ Å, and $V = 130.983(6)$ Å^3.

The *in situ* high-pressure XRD data were collected up to 15 GPa at room temperature. Selected XRD patterns are plotted in Fig. 2, where all peaks can be indexed into the C23-type Co_2P and B1-type NaCl. All peaks shift to higher angles of 2θ with pressure increasing. No peaks merged and no new peaks appear at pressures up to 15 GPa, implying that C23-type Co_2P is still stable in the present pressure range. At the highest pressure of 15 GPa, the whole sample was heated to a temperature of (1800 ± 200) K by a portable laser heating system, from one side diamond. Subsequently Co_2P was immediately quenched to room temperature by turning off the power of the laser. Finally the other side sample was also heated under the same conditions. After laser heating twice, the quenched product at 15 GPa was characterized by XRD (Fig. 2, curve *c*). The XRD pattern from high-temperature quenching is similar to that before laser heating. The result demonstrates that the C23-type Co_2P is still stable, even subject to high temperature at 15 GPa.

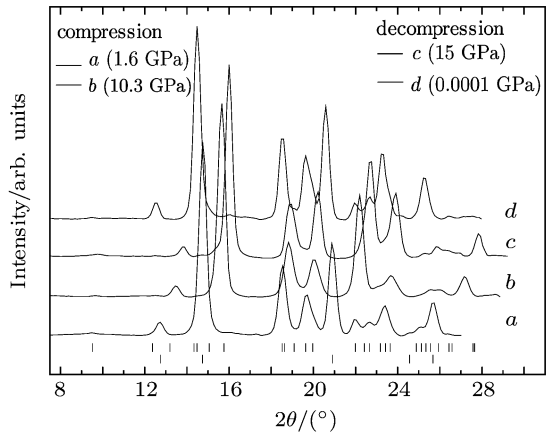


Fig. 2. Some selected X-ray diffraction patterns at high pressures. Their backgrounds were subtracted. Vertical bars represent the positions of diffraction peaks, which are assigned to the C23-type Co_2P and B1-type NaCl at 1.6 GPa.

Listed in Table 1 are lattice parameters of Co_2P on compressing and on decompressing. The individual unit-cell parameter and the volume show a smooth decrease with pressure increasing. Unit-cell volume as a function of pressure was analysed by the three-order Birch–Murnaghan EoS[21] using the Eosfit52 software.[22] The pressure derivative K_0' of -0.176 was obtained if no constrain was set during the fitting process. This value is not of physical significance obviously. Therefore we selected the second-order Birch–Murnaghan EoS to fit the P–V relationship with a fixed K_0' of 4. Parameters of the isothermal EoS were obtained as follows: $V_0 = 130.99(2)$ Å^3 and $K_0 = 160(3)$ GPa.

Axial compressibilities of the C23-type Co_2P were also described by the second-order Birch–Murnaghan (B–M) EoS:

$$P = \frac{K_d}{K_d'}\left[\left(\frac{d_0^3}{d^3}\right)^{K_d'} - 1\right],$$

where d_0 is the value of the unit-cell axis at room pressure, K_d is the compressional modulus of the axis and K_d' is equal to 4. Here we obtain $a_0 = 5.6511(4)$ Å and $K_a = 123(2)$ GPa, $b_0 = 3.5092(4)$ Å and $K_b = 167(8)$ GPa, $c_0 = 6.6051(4)$ Å and $K_c = 220(7)$ GPa (Fig. 3(a)). There is a distinctive anisotropy for the unit-cell compressibilities that the *a* axis is most compressible and the *c* axis is least compressible.

Table 1. Unit-cell parameters of Co_2P at various pressures.

P/GPa	a/Å	b/Å	c/Å	V/Å^3	
0.0001	5.6510 (2)	3.5090 (1)	6.6054 (2)	131.983 (6)	
1.6 (1)	5.641 (3)	3.501 (2)	6.600 (3)	130.3 (1)	
3.0 (3)	5.624 (5)	3.483 (3)	6.579 (5)	128.9 (1)	
4.3 (2)	5.597 (4)	3.474 (2)	6.561 (4)	127.6 (1)	
5.5 (5)	5.571 (6)	3.462 (4)	6.554 (9)	126.4 (1)	Compression
6.8 (1)	5.559 (3)	3.456 (2)	6.542 (4)	125.7 (1)	
8.3 (1)	5.545 (4)	3.452 (3)	6.525 (5)	124.9 (1)	
10.0 (3)	5.518 (6)	3.442 (4)	6.515 (7)	123.7 (1)	
11.6 (1)	5.501(4)	3.432 (3)	6.497 (6)	122.7 (1)	
12.5 (1)	5.498 (6)	3.427 (6)	6.481 (10)	122.1 (2)	
13.2 (2)	5.492 (7)	3.424 (6)	6.473 (10)	121.7 (2)	
14.9 (2)	5.463 (5)	3.422 (2)	6.458 (6)	120.7 (1)	
13.4 (1)	5.480 (4)	3.426 (2)	6.475 (5)	121.6 (1)	
12.7 (1)	5.490 (4)	3.430 (3)	6.493 (5)	122.3 (1)	
10.9 (0)	5.512 (5)	3.443 (4)	6.516 (6)	123.6 (1)	Decompression
9.6 (1)	5.515 (5)	3.454 (2)	6.531 (4)	124.4 (1)	
8.1 (2)	5.527 (5)	3.464 (2)	6.550 (5)	125.4 (1)	
6.3 (1)	5.562 (5)	3.473 (2)	6.549 (5)	126.5 (1)	
4.7 (0)	5.591 (3)	3.490 (1)	6.562 (4)	128.0 (1)	
3.2 (1)	5.617 (4)	3.494 (2)	6.583 (4)	129.2 (1)	
0.0001	5.647 (3)	3.516 (1)	6.604 (4)	130.9 (1)	

Note: The numbers in parentheses are the estimated standard deviations in units of the last digit.

3.2. The *ab initio* calculations

In the C23-type model, the LSDA calculations without plus U yield $K_0 = 242$ GPa and $V_0 = 120.78$ Å^3. The discrepancies are huge compared with theoretical and experimental results, meaning that the present calculation model cannot describe the real behaviour of Co_2P. Thus the LSDA+U calculations were adopted. New parameters of EoS were obtained as follows: $V_0 = 126.13$ Å^3, $K_0 = 186.3$ GPa, and $K_0' = 3.39$, which are in agreement with experimental values (Fig. 3(b)). Figure 4 displays the total energies each as a function of the volume for C22 and C23 phases. Our theoretical calculations indicate that the C23-type phase has a lower energy than the C22-type phase in various volumes. According to the relative Gibbs free energy as a function of pressure (the inset of Fig. 4), there is no possibility of phase transition from C23 to C22 at high pressure and low temperature.

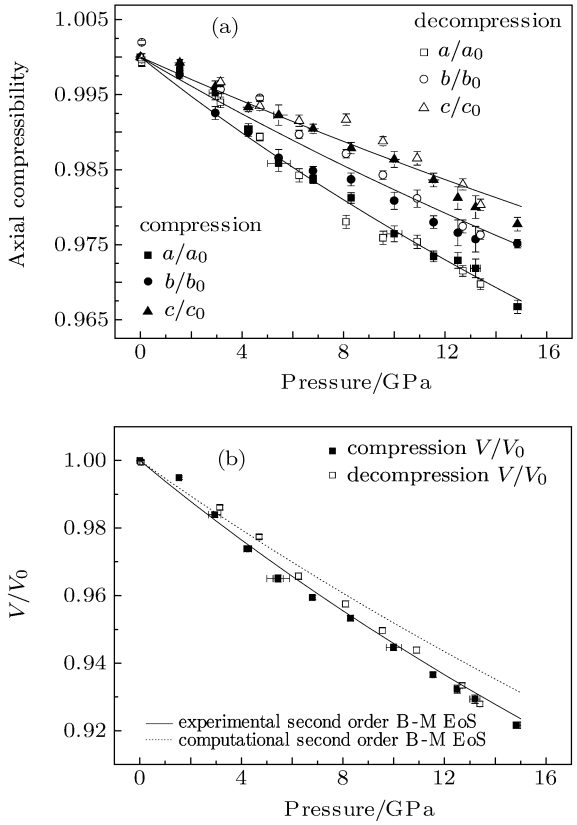


Fig. 3. Compressibility of the C23-type Co_2P. (a) Pressure dependence of normalized unit-cell parameters and (b) experimental and computational V/V_0 values of Co_2P as a function of pressure. Solid symbols show experimental data of compression, open symbols denote experimental data of decompression.

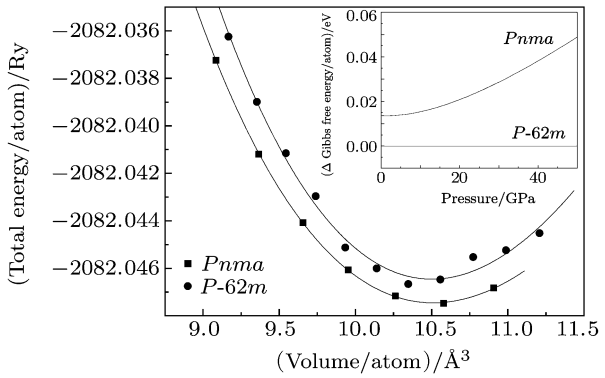


Fig. 4. Curves for calculated total energy versus volume for the two phases Co_2P: C23 and C22. The inset shows calculated relative Gibbs free energy with respect to that of the C23 versus pressure.

It is well known that the magnetic property of material is suppressed at high pressure. Figure 5 displays the computed magnetic moments each as a function of pressure for the C23 and the C22 structures. It is clear that the magnetic moment of Co1 with CN=5 is larger than that of Co2 with CN=4. In the C22 phase there is a magnetic collapse at about 16 GPa. However, no discontinuity is observed in the C23 phase. At above 16 GPa, the magnetic moments of Co2 become very small in both phases. This kind of magnetic moment behaviour of Co_2P at high pressure is very similar to that of Fe_2P.[23]

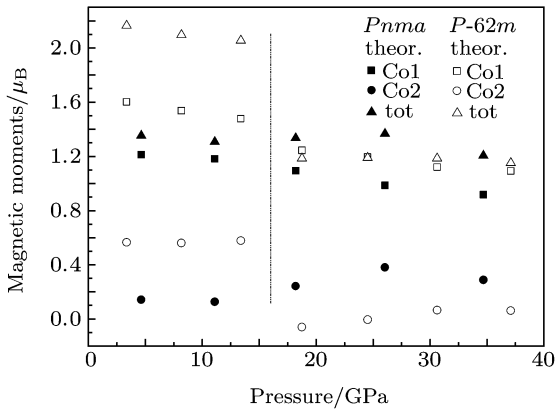


Fig. 5. Magnetic moments each as a function of pressure for the C23 and the C22. Co1 with CN=5 and Co2 with CN=4.

Available experimental and theoretical EoS parameters are listed in Table 2 for comparison. The equilibrium volume (V_0) obtained from theoretical computation is underestimated compared with those of experimental results, which is typical for the LDA computations. Isothermal bulk modulus of C23-type M_2P compounds are approximate. Overall, in the C22-type M_2P compounds, isothermal bulk modulus increases with V_0 decreasing.

Table 2. Parameters of EoS (V_0: volume per primitive cell at zero pressure).

M_2P	Phase	K_0/GPa	K_0'	V_0/Å^3	Reference
Fe_2P	C22	174(7)	4.0 (fixed)	34.38	DAC exp. [5]
Fe_2P	C22	165(3)	4.0 (fixed)	34.32	DAC exp. [24]
Fe_2P	C22	196	5.1	31.59	LDA + U [23]
Co_2P	C22	221.2	3.2	31.51	LDA + U [this study]
Ni_2P	C22	201(8)	4.2(6)	33.51 (fixed)	DAC exp. [7]
Fe_2P	C23	177(3)	4.0 (fixed)	34.48	DAC exp. [5]
Fe_2P	C23	184	6.7	31.03	LDA + U [23]
Co_2P	C23	160(3)	4.0 (fixed)	32.75	DAC exp. [this study]
Co_2P	C23	186.3	3.4	31.53	LDA + U [this study]

Both experimental and theoretical results confirm that the C23-type Co_2P is stable at pressures up to 15 GPa. It suggests that only pressure cannot induce the C23-to-C22 transformation in Co_2P. Dera *et al.*[5] studied the pressure-induced phase transformation of C22-type Fe_2P and observed that it transformed into the C23-type polymorph on heating to 1000 K above 8 GPa. At higher pressure Japel *et al.*[6] reported that C22-type Fe_2P transformed to a new, possibly monoclinic structure between 30 GPa and 50 GPa without observing C23 phase. Ni_2P with the C22-type phase remains stable to at least 50 GPa and room temperature.[7] Even plus our present results of Co_2P, the general rule of structural stabilities for M_2P compounds is still unclear.

4. Conclusions

The structure stability of Co_2P at high pressure is investigated by XRD and theoretical calculations. No phase transition is observed at up to 15 GPa and high temperature in the XRD experiments. The unit-cell compressibilities of the C23-type Co_2P represent an evident anisotropy, namely, the a axis is most compressible and the c axis is least compressible. Our *ab initio* calculations based on DFT within the LSDA+U show that the C23-type Co_2P remains stable at high pressure and low temperature. EoS parameters of the C23-type Co_2P are consistent with those obtained from experimental measurements and theoretical computations.

Acknowledgement

The authors would like to thank L Dubrovinsky for his assistance in high-temperature and high-pressure experiments and also X Wu for his Alexander von Humboldt Fellowship.

References

[1] Severin L, Häggström L, Nordström L andersson Y and Johansson B 1995 *J. Phys.: Condens. Matter* **7** 185

[2] Fujii S, Ishida S and Asano S 1988 *J. Phys.* F: *Met. Phys.* **18** 971

[3] Cai J W, Luo H L and Zheng Q Q 1993 *J. Phys.: Condens. Matter* **5** 9307

[4] Britvin S N, Rudashevsky N S, Krivovichev S V, Burns P C and Polekhovsky Y S 2002 *Am. Mineral.* **87** 1245

[5] Dera P, Lavina B, Borkowski L A, Prakapenka V B, Sutton S R, Rivers M L, Downs R T, Boctor N Z and Prewitt C T 2008 *Geophys. Res. Lett.* **35** L10301

[6] Japel S, Prewitt C and Boctor N 2002 *Am. Geophys. Union, Spring Meeting*, Washington DC, May 2002, abstract M51A-02

[7] Dera P, Lavina B, Borkowski L A, Prakapenka V B, Sutton S R, Rivers M L, Downs R T, Boctor N Z and Prewitt C T 2009 *J. Geophys. Res.* **114** B03201

[8] Rundqvist S 1960 *Acta Chem. Scand.* **14** 1961

[9] Parthé E, Gelato L, Chabot B, Penzo M, Cenzual K and Gladyshevskii R 1994 *TYPIX; Standardized Data and Crystal Chemical Characterization of Inorganic Structure Types*, Vol. 3 (Berlin: Springer-Verlag) p. 1050

[10] Zemczuzny S, Schepelew J and Anorg Z 1909 *Chem.* **64** 245

[11] De Vos K J, Welge W A J J, van der Steeg M G and Zijlstra H 1962 *J. Appl. Phys.* **33** 1320

[12] Massalski T B, Okamoto H, Subramanian P R and Kacprzak L 1990 *Binary Alloy Phase Diagrams* 2nd edn. Vol. 2, ASM International, The Materials Information Society, p. 1217
[13] Ishida K and Nishizawa T 1990 *Bull. Alloy Phase Diagrams* **11** 555
[14] Mao H K, Xu J and Bell P M 1986 *J. Geophys. Res.* **91** 4673
[15] Birch F 1986 *J. Geophys. Res.* **91** 4949
[16] Dubrovinsky L, Glazyrin K, McCammon C, Narygina O, Greenberg E, Uebelhack S, Chumakoy A I, Pascarelli S, Prakapenka V, Bock J and Dubrovinskain N 2009 *J. Synchrotron Rad.* **16** 737
[17] Blaha P, Schwarz K, Madsen G K H, Kvasnicka D and Luitz J 2002 *WIEN2k, An Augmented Plane Wave + Local Orbitals Program for Calculating Crystal Properties* revised edition June 2002, Prof. Dr. Karlheinz Schwarz, Technische Universität Wien, Institut für Physikalische und Theoretische Chemie, Getreidemarkt 9/156 A-1060 Wien/Austria
[18] Schwarz K, Blaha P and Madsen G K H 2002 *Comput. Phys. Commun.* **147** 71
[19] Pickett W E, Erwin S C and Ethridge E C 1998 *Phys. Rev.* B **58** 1201
[20] Skála R and Drábek M 2001 *Bulletin Czech Geological Survey* **76** 209
[21] Birch F 1952 *J. Geophys. Res.* **95** 227
[22] Angel R J 2001 *Rev. Mineral. Geochem.* **41** 35
[23] Wu X and Qin S 2010 *J. Phys.: Conf. Ser.* **215** 012110
[24] Scott H P, Kiefer B, Martin C D, Boateng N, Frank M R and Meng Y 2008 *High Pressure Res.* **28** 375